

Fig. 4. (Left) YUCCA is involved in tryptophan-dependent auxin biosynthesis, and the YUCCA pathway is functional in other plants. **(A)** *yucca* is less sensitive to toxic tryptophan analogs. Wild-type (left) and *yucca* seedlings were grown on 0.5X MS medium containing 100- μ M 5-mT for 10 days. **(B)** Comparison of wild-type (left) and transgenic tobacco plants overexpressing YUCCA. **Fig. 5. (Right)** YUCCA catalyzes a key step in auxin biosynthesis. Putative tryptophan-dependent auxin biosynthesis pathways and intermediates are shown (2). The indole-3-acetaldoxime intermediate was proposed recently (25).

may yield additional clues that can be used to elucidate the physiological roles of their mammalian counterparts.

References and Notes

1. P. J. Davies, Ed., in *Plant Hormones: Physiology, Biochemistry and Molecular Biology*, (Kluwer Academic, Dordrecht, Netherlands, 1995), pp. 1–12.
2. B. Bartel, *Annu. Rev. Plant Physiol. Plant Mol. Biol.* **48**, 51 (1997).
3. _____, G. R. Fink, *Proc. Natl. Acad. Sci. U.S.A.* **91**, 6649 (1994).
4. D. Bartling, M. Seedorf, A. Mithofer, E. W. Weiler, *Eur. J. Biochem.* **205**, 417 (1992).
5. J. Normanly, P. Grisafi, G. R. Fink, B. Bartel, *Plant Cell* **9**, 1781 (1997).
6. R. C. Schmidt, A. Muller, R. Hain, D. Bartling, E. W. Weiler, *Plant J.* **9**, 683 (1996).
7. J. J. King, D. P. Stimart, R. H. Fisher, A. B. Bleecker, *Plant Cell* **7**, 2023 (1995).
8. M. Delarue, E. Prinsen, H. V. Onckelen, M. Caboche, C. Bellini, *Plant J.* **14**, 603 (1998).
9. W. Boerjan et al., *Plant Cell* **7**, 1405 (1995).
10. A. Lehman, R. Black, J. R. Ecker, *Cell* **85**, 183 (1996).
11. J. L. Celenza Jr., P. L. Grisafi, G. R. Fink, *Genes Dev.* **9**, 2131 (1995).
12. D. Weigel et al., *Plant Physiol.* **122**, 1003 (2000).
13. C. P. Romano, P. R. Robson, H. Smith, M. Estelle, H. Klee, *Plant Mol. Biol.* **27**, 1071 (1995).
14. R. J. Pitts, A. Cernac, M. Estelle, *Plant J.* **16**, 553 (1998).
15. Analysis of free auxin was done as described by K. Chen, A. N. Miller, G. W. Patterson, and J. D. Cohen [*Plant Physiol.* **86**, 822 (1988)]. Six-day-old *yucca* and wild-type seedlings grown in 0.5X MS medium at 22°C in white light were used for the analysis.
16. J. Mathur, C. Koncz, in *Arabidopsis Protocols*, J. M.

Martinez-Zapater, J. Salinas, Eds. (Human Press, Totowa, NJ, 1998), vol. 82, pp. 31–34.

17. S. Sabatini et al., *Cell* **99**, 463 (1999).
18. C. P. Romano, M. B. Hein, H. J. Klee, *Genes Dev.* **5**, 438 (1991).
19. D. M. Ziegler, *Drug Metab. Rev.* **19**, 1 (1988).

20. J. R. Cashman, *Chem. Res. Toxicol.* **8**, 165 (1995).
21. Y. Zhao, J. Chory, unpublished data.
22. Y. Zhao, S. Christensen, D. Weigel, J. Chory, unpublished data.
23. Y. Zhao, S. Christensen, J. Alonso, J. Ecker, J. Chory, unpublished data.
24. Y. Zhao, M. Neff, J. Chory, unpublished data.
25. A. K. Hull, R. Vij, J. L. Celenza, *Proc. Natl. Acad. Sci. U.S.A.* **97**, 2379 (2000).
26. Transformation of tobacco was carried out as described by P. Gallois and P. Marinho [*Methods Mol. Biol.* **49**, 39 (1995)].
27. N. B. Beaty, D. P. Ballou, *J. Biol. Chem.* **256**, 4619 (1981).
28. _____, *J. Biol. Chem.* **256**, 4611 (1981).
29. Recombinant YUCCA was purified from *Escherichia coli* as a maltose binding protein (MBP) fusion according to the procedures for expressing human FMOs [A. Brunelle et al., *Drug Metab. Dispos.* **25**, 1001 (1997)]. For activity assays, 350 μ g of YUCCA-MBP was incubated with 2 mM tryptamine, 1 mM NADP⁺, 1 mM glucose-6-phosphate, and 2.0 IU of glucose-6-phosphate dehydrogenase in 120- μ L total volume at 37°C for 3 hours. The reactions were stopped by adding an equal volume of methanol. The substrate and products were separated by thin-layer chromatography (TLC) with CH₂Cl₂/methanol/tetraethylammonium (TEA) (75:20:5). The product was eluted from the TLC plates, and Electrospray mass spectrometry was performed under positive mode to determine the molecular mass of the product.
30. Y. Zhao, J. R. Cashman, J. Chory, unpublished data.
31. We thank M. Estelle for providing *iaaL* overexpression *Arabidopsis* lines, L. Barden for assistance with the art work, T. Dabi for help with tobacco transformation, and J. Perry and members of the Chory lab for useful comments. Supported by grants from NIH (2R01GM52413) and NSF (MCB9631390) to J.C., from NSF (MCB 9723823) to D.W., from NIH (R01GM36426) to J.R.C., from DOE (DE-FG02-00ER15079) and from Minnesota Agricultural Experiment Station and the Bailey Endowment for Environmental Horticulture to J.D.C., and from the Howard Hughes Medical Institute. Y.Z. is a HHMI Fellow of the Life Sciences Research Foundation; S.C. was partially supported by an NSF fellowship; C.F. was a fellow of the Human Frontier Science Program and the Swiss NSF. J.C. is an Associate Investigator of the HHMI.

12 October 2000; accepted 1 December 2000

Transgenic Monkeys Produced by Retroviral Gene Transfer into Mature Oocytes

A. W. S. Chan, K. Y. Chong, C. Martinovich, C. Simerly, G. Schatten*

Transgenic rhesus monkeys carrying the green fluorescent protein (GFP) gene were produced by injecting pseudotyped replication-defective retroviral vector into the perivitelline space of 224 mature rhesus oocytes, later fertilized by intracytoplasmic sperm injection. Of the three males born from 20 embryo transfers, one was transgenic when accessible tissues were assayed for transgene DNA and messenger RNA. All tissues that were studied from a fraternal set of twins, miscarried at 73 days, carried the transgene, as confirmed by Southern analyses, and the GFP transgene reporter was detected by both direct and indirect fluorescence imaging.

Although transgenic mice have been invaluable in accelerating the advancement of biomedical sciences (1–5), many differences between humans and rodents have limited their

usefulness (6–9). The major obstacle in producing transgenic nonhuman primates has been the low efficiency of conventional gene transfer protocols. By adapting a pseu-

REPORTS

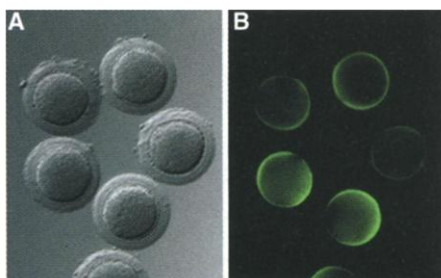


Fig. 1. Injection of VSV-G pseudotyped retroviral vector, enclosing the GFP gene and protein, into the perivitelline space of mature rhesus oocytes. (A) Transmitted light and (B) epifluorescence imaging of GFP carried within the vector particles. Magnification: $\times 100$.

dotyped vector system, efficient at up to 100% in cattle (10, 11), we circumvented problems in traditional gene transfer methodology to produce transgenic primates.

We injected 224 mature rhesus oocytes with high titer [10^8 to 10^9 colony-forming units (cfu/ml)] moloney retroviral vector pseudotyped with vesicular stomatitis virus envelope glycoprotein G (VSV-G pseudotype) into the perivitelline space (Fig. 1; Table 1; 10–12). The VSV-G pseudotype carried the GFP gene under the control of either the cytomegalovirus early promoter (CMV) [referred to as LNCEGFP-(VSV-G)] or the human elongation factor-1 alpha promoter (hEF-1 α) [referred to as LNEFEGFP-(VSV-G)] (13). Because ~ 10 to 100 pl was introduced into the perivitelline space, between 1 and 10 vector particles were introduced using LNCEGFP-(VSV-G) [10^9 cfu/ml] and between 0.1 to 1 with LNEFEGFP-(VSV-G) (10^8 cfu/ml). Oocytes were cultured for 6 hours before fertilization by intracytoplasmic sperm injection (ICSI). Vector particles incorporated into the oocyte in <4.5 hours as imaged by electron microscopy (14). Fifty-seven percent ($n = 126$) of embryos developed beyond the four-cell stage and 40 embryos were transferred to 20 surrogates, each carrying two embryos (Table 1). Rates for reproductive parameters are: fertilization [77% ICSI controls (15) versus 75% transgenesis], embryonic development [75% ICSI controls (15) versus 57% transgenesis], and implantation [66% ICSI controls (16) versus 25% transgenesis]. Most control ICSI pregnancies result in live offspring (83%) (16).

Five pregnancies resulted in the births of three healthy males (Table 1, Fig. 2). A set of

Oregon Regional Primate Research Center, Center for Women's Health, and Departments of Cell-Developmental Biology and Obstetrics-Gynecology, Oregon Health Sciences University, 505 NW 185th Avenue, Beaverton, OR 97006, USA.

*To whom correspondence should be addressed. E-mail: schatten@ohsu.edu

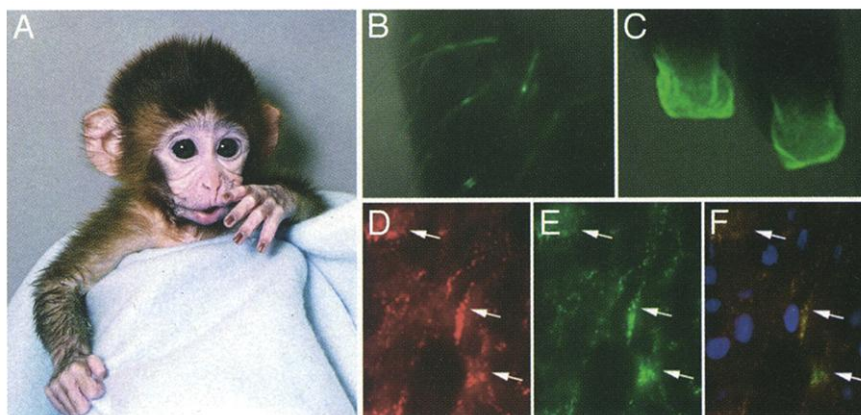


Fig. 2. (A) Transgenic rhesus male with inserted DNA ("ANDi"). GFP expression was observed in hair shafts (B) and toenails (C) by direct epifluorescent examination in the male stillborn but not in the accessible tissues from ANDi. Immunostaining and epifluorescent examination of placental frozen sections from the male stillborn demonstrates the presence of the GFP protein. (D) Anti-GFP detection in placenta by rhodamine (red) immunofluorescent microscopy. (E) GFP detection by fluorescein (green) epifluorescence of the same section demonstrates the direct expression of the transgene. (F) Overlay of the green (E) and red (D) images demonstrates colocalization of direct GFP fluorescence with anti-GFP imaging. Blue, Hoechst 33342 DNA staining. Magnification in (D) through (F): $\times 400$.

Table 1. Transgenesis efficiency in rhesus embryos, fetuses, and offspring.

Construct	VSV-G pseudotype		Overall
	LNCEGFP	LNEFEGFP	
Eggs injected with vector	157	67	224
Eggs then injected with sperm	157	65	222
Fertilization rate	108 (69%)	58 (89%)	166 (75%)
Embryonic development of fertilized eggs	85 (79%)	41 (71%)	126 (76%)
Embryos transferred (two/surrogate)	22	18	40
Number of surrogates	11	9	20
Pregnancies/surrogate	1* (9%)	4 (44%)	5 (25%)
Fetal losses	2 (100%)	1 (25%)	3 (50%)
Births	0	3	3
Transgenic	2 of 2	1 of 4	3 of 6
Transgenic birth/embryos transferred	0	1 (5.5%)	1 (2.5%)
Transgenic birth/pregnancies	0	1 (25%)	1 (20%)

*Twin pregnancy.

fraternal twins miscarried at 73 days (150 to 155 days normal gestation) and a blighted pregnancy (implantation attempt without a fetus) also occurred. One fetal twin of the miscarriage was an anatomically normal male, while the other was largely resorbed in utero. The three births and the blighted pregnancy resulted from nine embryo transfers in which LNEFEGFP-(VSV-G) was used, whereas the twin pregnancy was established from 11 embryo transfers with LNCEGFP-(VSV-G) (Table 1).

Transgene integration, transcription, and expression from the newborns were examined in hair, blood, umbilical cords, placenta, cultured lymphocytes, buccal epithelial cells, and urogenital cells passed in urine, along with 13 tissues from the male stillborn, nine from the resorbed one, and specimens from the blighted pregnancy (17). Polymerase chain reaction (PCR) was performed with primer sets that covered the flanking region of the vector pLNC-EGFP or pLNEF-EGFP and the GFP

gene (18). One newborn, ANDi, showed the presence of the transgene in all analyzed tissues, and the transgene was present in all tissues analyzed from both stillbirths including placenta and testes (Fig. 3). Total RNA was extracted for standard reverse transcription followed by PCR amplification (RT-PCR) with primer sets specific for the transgene (18). Transgene transcription was demonstrated in all of the tissues in the fetuses and in the accessible tissues from the infant carrying the transgene (Fig. 3).

Southern blot analysis of 10 tissues from the male stillbirth and eight samples from the other twin demonstrated multiple integration sites into their genomic DNA (Fig. 4) (19). Vector integration was determined by PCR of placenta, cord, blood, hair, and buccal cells using a primer set specific for the unique retroviral long terminal repeat (LTR) regions indicative of successful provirus integration into the host genome (20, 21). This provirus sequence was found in one infant and both

REPORTS

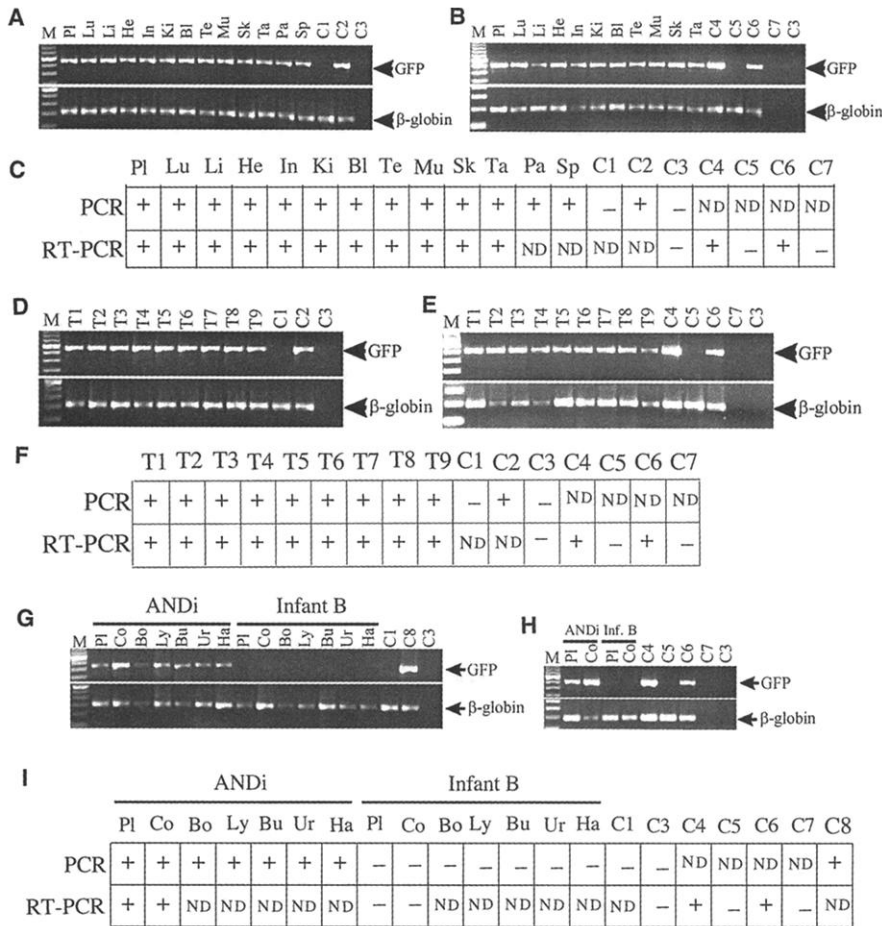


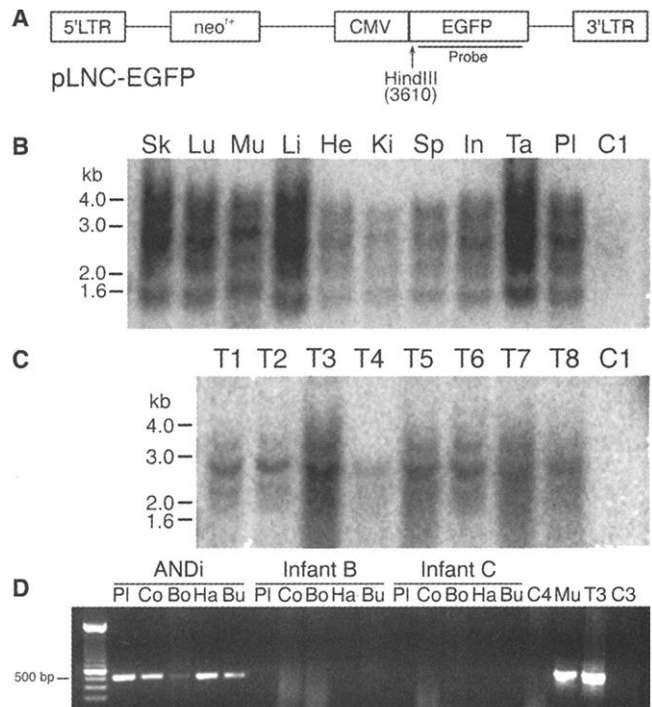
Fig. 3. PCR and RT-PCR analyses of transgenic and control tissues. (A) Thirteen tissues from an intact fetus were submitted for PCR and (B) 11 tissues for RT-PCR. (C) Analysis of the male stillborn. Tissues from the reabsorbed fetus were collected from eight different regions to ensure broad representation, because precise anatomical specification was limited. (D through F) PCR, RT-PCR of the reabsorbed fetus. A total of seven samples were obtained from each offspring for PCR (G), two samples for RT-PCR (H) from "ANDi" and one of the other two male offspring. (I) Analysis of the newborns, indicates that "ANDi" is a transgenic male with the presence of mRNA in all analyzed tissues. Co, cord; Bo, blood; Ly, lymphocyte; Bu, buccal cells; Ur, urine; Ha, hair; Pl, placenta; Lu, lung; Li, liver; He, heart; In, intestine; Ki, kidney; Bl, bladder; Te, testis; Mu, muscle; Sk, skin; Ta, tail; Pa, pancreas; Sp, spleen; T1 = placenta from reabsorbed fetus; T2 to T9 = tissues retrieved from eight regions of the reabsorbed fetus; C1 = nontransgenic rhesus tissue; C2 = C1 + pLNC-EGFP; C3 = ddH₂O; C4 = 293GP-LNCEGFP packaging cell; C5 = nontransgenic liver; C6 = transgenic lung without DNase; C7 = transgenic lung without reverse transcription; C8 = C1 + pLNEF-EGFP. ND, not determined.

stillbirths (Fig. 4D). Infant welfare considerations limited tissue availability, and genomic DNA obtained was insufficient for Southern analysis. The male infant with the inserted transgene has been named "ANDi" (for "inserted DNA," in a reverse transcribed direction; Fig. 2A).

GFP direct fluorescence in the toenails and hair of the fetus, as well as the placenta (Fig. 2, B through F), provided further evidence of transgenesis. Colocalization between direct GFP fluorescence and indirect anti-GFP immunocytochemical imaging demonstrated that the GFP protein is found exclusively at the direct fluorescence sources (Fig. 2, D through F). Furthermore, neither direct fluorescein nor indirect rhodamine fluorescence was observed in controls (22). Because tissues from the fetus originated from the three germ layers, the timing of transgene integration may have occurred before implantation, perhaps even before the first DNA replication cycle (10). The high efficiency of this approach has been linked to the absence of the nuclear envelope in oocytes naturally arrested in second meiotic metaphase (10, 23).

The miscarriage is likely due to the twin pregnancy, which is rare and high-risk in rhesus. The twin stillbirth originated from the

Fig. 4. (A) Southern blot analysis of Hind III (single digestion site) digested genomic DNA. Full-length GFP labeled with [³²P] was used as a probe to detect the transgene, which was detected in genomic DNA of the normal male stillbirth (B) and reabsorbed fetus (C). Nontransgenic rhesus tissue was used as a negative control (C1) and pLNC-EGFP DNA as a positive control (not shown). Various sized fragments were demonstrated in tissues obtained from each. This result indicates multiple integration sites due to the use of a restriction enzyme with a single digestion site within the transgene. (D) Detection of the unique provirus sequence. A total of five tissues from each infant and two tissues from a male stillbirth and the reabsorbed fetus were submitted for PCR. Provirus sequence was detected in "ANDi" and the two stillbirths (42), which indicates that they are transgenic. Abbreviations are the same as those in Fig. 3. Mu, muscle from the male stillbirth; T3, tissue from the reabsorbed fetus.



higher titer vector, whereas the three births, including the transgenic one, and the blighted pregnancy originated from the lower titer LNEFEGFP-(VSV-G) vector (10^8 cfu/ml; Table 1). Although only one live offspring is shown to be transgenic, we cannot yet exclude the possibility of transgenic mosaics in the others. We have neither demonstrated germline transmission nor the presence of transgenic sperm; this must await ANDi's development through puberty in about 4 years. Vector titers and volume injected may play crucial roles in gene transfer efficiency. These offspring and their surrogates are now housed in dedicated facilities with ongoing, stringent monitoring.

Nonhuman primates are invaluable models for advancing gene therapy treatments for diseases such as Parkinson's (24) and diabetes (25), as well as ideal models for testing cell therapies (26) and vaccines, including those for HIV (27, 28). Although we have demonstrated transgene introduction in rhesus monkeys, significant hurdles remain for the successful homologous recombination essential for gene targeting (29). The molecular approaches for making clones [either by embryo splitting (30) or nuclear transfer (31–36)], utilizing stem cells (37–39), and now producing transgenic monkeys, could be combined to produce the ideal models to accelerate discoveries and to bridge the scientific gap between transgenic mice and humans.

References and Notes

1. M. J. Blouin *et al.*, *Nature Med.* **6**, 177 (2000).
2. R. L. Eckert *et al.*, *Int. J. Oncol.* **16**, 853 (2000).
3. H. M. Hsieh-Li *et al.*, *Nature Genet.* **24**, 66 (2000).
4. A. M. Murphy *et al.*, *Science* **287**, 488 (2000).
5. E. J. Weinstein *et al.*, *Mol. Med.* **6**, 4 (2000).
6. J. A. Thomson, V. S. Marshall, *Curr. Topics Dev. Biol.* **38**, 133 (1998).
7. A. W. S. Chan *et al.*, *Mol. Hum. Reprod.* **6**, 26 (2000).
8. K. R. Chien, *J. Clin. Invest.* **98**, S19 (1996).
9. R. P. Erickson, *BioEssays* **18**, 993 (1996).
10. A. W. S. Chan *et al.*, *Proc. Natl. Acad. Sci. U.S.A.* **95**, 14028 (1998).
11. J. K. Yee *et al.*, *Methods Cell Biol.* **43**, 99 (1994).
12. The GFP vector was injected into the perivitelline space (10) of *in vivo* matured rhesus oocytes (40), fertilized by ICSI 6 hours later. Embryos at the four- to eight-cell stage were selected for embryo transfer on the basis of morphology. Surrogate females were selected on the basis of serum estradiol and progesterone levels (15).
13. The GFP gene from plasmid pEGFP-N1 was inserted into the retroviral vector pLNCX using standard recombinant DNA techniques [Web supplement 1 (41)].
14. Oocytes for electron microscopy were fixed in Ito-Karnovsky's fixative [Web supplement 2 (41)].
15. L. Hewitson *et al.*, *Hum. Reprod.* **13**, 2786 (1998).
16. L. Hewitson *et al.*, *Nature Med.* **5**, 431 (1999).
17. Genomic DNA was extracted from tissues obtained from the stillbirths [Web supplement 3 (41)].
18. PCR was performed using specific primers that amplify the flanking region of the GFP gene. Provirus was detected by using a primer set specific to the unique LTR region of genomic integrated virus. Transgene was detected by standard reverse transcription followed by PCR [Web supplement 4 (41)].
19. Southern analysis was performed using genomic DNA followed by restriction enzyme digestion using a

- unique site within the vector and detected by a GFP [³²P]-labeled probe [Web supplement 5 (41)].
20. B. Schott *et al.*, *Nucleic Acid Res.* **25**, 2940 (1997).
21. N. Chinnasamy *et al.*, *Hum. Gene Ther.* **11**, 1901 (2000).
22. Biopsied tissues were snap frozen, sectioned, fixed, and imaged with anti-GFP using rhodamine-conjugated anti-mouse (IgG) secondary antibody [Web supplement 6 (41)].
23. T. Roe *et al.*, *EMBO J.* **12**, 2099 (1993).
24. J. H. Kordower *et al.*, *Science* **290**, 767 (2000).
25. H. C. Lee *et al.*, *Nature* **408**, 483 (2000).
26. D. H. Barouch *et al.*, *Proc. Natl. Acad. Sci. U.S.A.* **97**, 4192 (2000).
27. M. J. Kuroda *et al.*, *J. Virol.* **74**, 8751 (2000).
28. N. Nathanson *et al.*, *AIDS (suppl. A)* **13**, S113 (1999).
29. U. Muller, *Mech. Dev.* **82**, 1 (1999).
30. A. W. S. Chan *et al.*, *Science* **287**, 317 (2000).
31. I. Wilmut *et al.*, *Nature* **385**, 810 (1997).
32. J. B. Cibelli *et al.*, *Science* **280**, 1256 (1998).
33. T. Wakayama *et al.*, *Nature* **394**, 369 (1998).
34. D. P. Wolf *et al.*, *Biol. Reprod.* **60**, 199 (1999).
35. A. Onishi *et al.*, *Science* **289**, 1188 (2000).
36. I. A. Polejaeva *et al.*, *Nature* **407**, 86 (2000).
37. J. A. Thomson *et al.*, *Proc. Natl. Acad. Sci. U.S.A.* **92**, 7844 (1995).

38. M. J. Shablott *et al.*, *Proc. Natl. Acad. Sci. U.S.A.* **95**, 13726 (1998).
39. J. A. Thomson *et al.*, *Science* **282**, 1145 (1998).
40. G. J. Wu *et al.*, *Biol. Reprod.* **55**, 269 (1996).
41. Supplementary figures are available at www.sciencemag.org/cgi/content/full/291/5502/309/DC1.
42. A. W. S. Chan, K. Y. Chong, C. Martinovich, C. Simerly, G. Schatten, data not shown.
43. We thank J. C. Burns (University of California San Diego); B. True (University of Wisconsin–Madison); K. Wells (U.S. Department of Agriculture); Chiron Inc.; and all at the Oregon Regional Primate Research Center (ORPRC), especially M. Axthelm, J. Bassir, J. M. Cook, N. Duncan, M. Emme, J. Fanton, A. Hall, L. Hewitson, D. Jacob, E. Jacoby, A. Lewis, C. M. Luetjens, C. Machida, G. Macginnis, B. Mason, T. Swanson, D. Takahashi, K. Tice, J. Vidgoff, M. Webb, and S. Wong. Procedures approved by the Oregon Health Sciences University/ORPRC Animal Care and Biosafety Committees. Supported by NIH/National Center for Research Resources (NCR) (ORPRC; M. S. Smith, Director) and grants (NCR, National Institute of Child Health and Human Development to G.S.).

7 November 2000; accepted 14 December 2000

Categorical Representation of Visual Stimuli in the Primate Prefrontal Cortex

David J. Freedman,^{1,2,5} Maximilian Riesenhuber,^{3,4,5} Tomaso Poggio,^{3,4,5} Earl K. Miller^{1,2,5*}

The ability to group stimuli into meaningful categories is a fundamental cognitive process. To explore its neural basis, we trained monkeys to categorize computer-generated stimuli as "cats" and "dogs." A morphing system was used to systematically vary stimulus shape and precisely define the category boundary. Neural activity in the lateral prefrontal cortex reflected the category of visual stimuli, even when a monkey was retrained with the stimuli assigned to new categories.

Categorization refers to the ability to react similarly to stimuli when they are physically distinct, and to react differently to stimuli that may be physically similar (1). For example, we recognize an apple and a banana to be in the same category (food) even though they are dissimilar in appearance, and we consider an apple and a billiard ball to be in different categories even though they are similar in shape and sometimes color. Categorization is fundamental; our raw perceptions would be useless without our classification of items as furniture or food. Although a great deal is known about the neural analysis of visual features, little is known about the neural basis of the categorical information that gives them meaning.

In advanced animals, most categories are learned. Monkeys can learn to categorize stimuli as animal or non-animal (2), food or non-food (3), tree or non-tree, fish or non-fish (4), and by ordinal number (5). The neural correlate of such perceptual categories might be found in brain areas that process visual form. The inferior temporal (IT) and prefrontal (PF) cortices are likely candidates; their neurons are sensitive to form (6–9) and they are important for a wide range of visual behaviors (10–12).

The hallmark of perceptual categorization is a sharp "boundary" (13). That is, stimuli from different categories that are similar in appearance (e.g., apple/billiard ball) are treated as different, whereas distinct stimuli within the same category (e.g., apple/banana) are treated alike. Presumably, there are neurons that also represent such sharp distinctions. This is difficult to assess with a small subset of a large, amorphous category (e.g., food, human, etc). Because the category boundary is unknown, it is unclear whether neural activity reflects category membership or physical similarity.

¹Center for Learning and Memory, ²RIKEN-MIT Neuroscience Research Center, ³Center for Biological and Computational Learning, ⁴McGovern Institute for Brain Research, ⁵Department of Brain and Cognitive Sciences, Massachusetts Institute of Technology, Cambridge, MA 02139, USA.

*To whom correspondence should be addressed. E-mail: ekm@ai.mit.edu